Structural Transients of Contractile Proteins upon Sudden ATP Liberation in Skeletal Muscle Fibers

Jun'ichi Wakayama,* Takumi Tamura,† Naoto Yagi,* and Hiroyuki Iwamoto*
*Life and Environment Division, SPring-8, Japan Synchrotron Radiation Research Institute, Hyogo 679-5198, Japan; and
†Structural Biochemistry Laboratory, RIKEN Harima Institute, SPring-8, Hyogo 679-5148, Japan

ABSTRACT Structural changes of contractile proteins were examined by millisecond time-resolved two-dimensional x-ray diffraction recordings during relaxation of skinned skeletal muscle fibers from rigor after caged ATP photolysis. It is known that the initial dissociation of the rigor actomyosin complex is followed by a period of transient active contraction, which is markedly prolonged in the presence of ADP by a mechanism yet to be clarified. Both single-headed (overstretched muscle fibers with exogenous myosin subfragment-1) and two-headed (fibers with full filament overlap) preparations were used. Analyses of various actin-based layer line reflections from both specimens showed the following: 1), The dissociation of the rigor actomyosin complex was fast and only modestly decelerated by ADP and occurred in a single exponential manner without passing through any detectable transitory state. Its ADP sensitivity was greater in the two-headed preparation but fell short of explaining the large ADP effect on the transient active contraction. 2), The decay of the activated state of the thin filament followed the time course of tension more closely in an ADP-dependent manner. These results suggest that the interplay between the reattached active myosin heads and the thin filament is responsible for the prolonged active contraction in the presence of ADP.

INTRODUCTION

Understanding how the actomyosin complex terminates its active force production is equally as important as understanding how it generates active force. In the MgATPase cycle of actomyosin, this termination step is generally assigned to the dissociation of the nucleotide-free (rigor) actomyosin complex upon ATP binding. This is a step in which a dramatic event takes place, i.e., through yet to be described structural changes at the actin-myosin interface, the binding constant of the complex is reduced from the greatest of all the intermediates to the smallest. In the presence of physiological concentrations of ATP, this reaction step is fast and is not rate limiting or synchronized. The synchronization of this reaction step had been a major hurdle to clear for studying the underlying molecular events by using muscle fibers.

Goldman and colleagues (Goldman et al., 1982, 1984a,b) pioneered in synchronizing the step by the flash photolysis of caged ATP, an inert precursor of ATP that is split upon irradiation with an ultraviolet (UV) pulse and releases ATP (Kaplan et al., 1978). They studied the changes in mechanical properties during the course of relaxation after photolysis. They made an important finding that, in the absence of calcium, the photolysis-induced relaxation consisted of two phases: 1), the initial dissociation of the rigor actomyosin complex that could be described in terms of second-order kinetics and 2), a transient active force generation that manifested itself as a transient hump of tension and the out-of-phase (viscous) component of muscle fiber stiffness. The second phase was later shown to be markedly prolonged in the presence of low ($\sim$50 μM) concentrations of ADP (Dantzig et al., 1991; Thirlwell et al., 1994). This tendency is more pronounced in cardiac muscle (Martin and Barsotti, 1994) and slow skeletal muscle (Horiuti et al., 1997). As for the mechanisms for this prolonged activity, the cooperative activation of the thin filament by rigor-like myosin heads has been considered responsible (Dantzig et al., 1991; Martin and Barsotti, 1994; Thirlwell et al., 1994). It has been proposed that the slower release of ADP from actomyosin prolongs the life of rigor-like myosin heads capable of thin filament activation (Martin and Barsotti, 1994). Thirlwell et al. (1994) have proposed that it is the ADP-bound form of actomyosin complex that is responsible for keeping the thin filament activated. However, conflicting evidence has been presented by Horiuti and Kagawa (1998), and the detailed mechanism remains to be clarified.

The structural changes of contractile proteins during the course of photolysis-induced relaxation may be studied by x-ray diffraction. However, the structural changes caused by the photolysis are fast (millisecond timescales) and require a high time resolution of recording. Some time-resolved x-ray recordings have been made by using synchrotron radiation (Goody et al., 1985; Poole et al., 1988, 1991; Horiuti et al., 1994, 1997, 2001; Tsaturyan et al., 1999; Yamada et al., 2003), but there have been limitations as to both time resolution and the number of reflections that can be analyzed. To understand fully the structural basis of the relaxation process, one should obtain the intensity profiles as well as the integrated intensities from as many actin-based

Submitted September 20, 2003, and accepted for publication March 19, 2004.

Address reprint requests to Dr. Hiroyuki Iwamoto, Life and Environment Division, SPring-8, Japan Synchrotron Radiation Research Institute, 1-1-1 Kouto, Mikazuki-cho, Sayo-gun, Hyogo 679-5198 Japan. Tel.: 81-791-58-2507; Fax: 81-791-58-0830; E-mail: iwamoto@spring8.or.jp.

J. Wakayama's present address is Structural Biochemistry Laboratory, RIKEN Harima Institute, SPring-8, Hyogo 679-5148, Japan.

0006-3495/04/07/430/12 $2.00

doi: 10.1529/biophysj.103.035063

layer line reflections (ALL's) as possible. Although most of them are much weaker and more diffuse than the previously studied more intense reflections, they carry important information about the structure of the actomyosin complex and the thin filament itself.

Here we were able to record the changes of these weak ALL's, up to the 7th ALL (1/5.1 nm^{-1}) and including the faint 2nd ALL outer part (1/19 nm^{-1}), during photolysis-induced relaxation at a time resolution of 3.4 ms by using the high-flux BL40XU beamline at SPring-8. In this beamline, a flux of 10^{15} photons/s (i.e., 10^3 times higher than in other undulator-based beamlines) is achieved by omitting the monochromator (Inoue et al., 2001).

As materials, two systems were used in this study. In the first system, skinned skeletal muscle fibers were stretched to a long sarcomere length, and exogenous myosin subfragment-1 (S1) was diffused into them. The diffused S1 molecules attach and fully decorate the endogenous thin filaments and form rigor complexes. By using this system, we address a question as to whether the S1 molecules simply dissociate from actin upon ATP binding or they adopt transient configurations (e.g., a disordered state or a conformation distinct from rigor) before the complex dissociates completely.

In the second system, skinned muscle fibers were held at a length with full filament overlap. This system is equivalent to that used for the previous mechanical measurements. By using this system we address questions as to 1), whether the two headedness of a myosin molecule affects the time course of rigor complex dissociation or its ADP dependence and 2), whether the large ADP effect on the active phase of relaxation is explained by the kinetics of rigor complex dissociation alone or other factors must be taken into consideration.

A part of these results has been presented in a preliminary form (Iwamoto et al., 2003b).

MATERIALS AND METHODS

Specimens, solutions, and experimental procedure

Single skinned muscle fibers were prepared from rabbit psoas as described previously (Iwamoto, 1995). About 30 single fibers were parallel aligned in each specimen chamber as described (Iwamoto et al., 2001). The ends of the fibers were clamped to the chamber by utilizing an electron microscopy grid split in half. The fibers were mounted while they were in a relaxing solution, and their sarcomere length was adjusted to either 2.4 μm (full filament overlap) or 3.3–3.5 μm (overstretched) by using He-Ne laser diffraction before they were transferred to a rigor solution containing 20 mM butanedione monoxime (BDM) to prevent the fibers from developing rigor force. Fibers at full filament overlap were stored in the rigor solution without BDM until the time of experiment (a few days) in a refrigerator. Overstretched fibers were stored in the same manner, but, ~24 h before the experiment, the solution was replaced by the one containing 2–3 mg/ml S1 prepared from rabbit skeletal muscle as described (Iwamoto et al., 2001).

Shortly before experiments, the solution in the specimen chamber was replaced by a photolysis solution containing caged ATP. The fibers were incubated in that solution for at least 5 min before photolysis. After the x-ray recording with photolysis, the fibers were flushed with a relaxing solution and subjected to another run of x-ray recording. The fibers were discarded at this point, because radiation damage would become apparent after further x-ray exposure.

Finally, the whole recording procedure was repeated once again with the experimental chamber filled with the caged ATP solution alone (without fibers). The images recorded in this way were subtracted from the diffraction patterns from corresponding frames. This procedure should correct the diffraction data for scattering from the solution, quartz windows, and the offset (dark current) inherent in each of the three charge-coupled device (CCD) chips in the detector (see below). After the recording, the solution was retrieved for analysis by high performance liquid chromatography (HPLC; model 600E, Waters, Milford, MA) to determine the concentration of photoreleased ATP. To estimate the concentration of photoreleased ATP in and around the fibers, a compartment was placed within the chamber so that the solution was confined to the area occupied by the fibers. The photoreleased ATP determined in this way was 1.8 mM.

The solutions had the following composition (in mM). The relaxing solution contained K-propionate, 80; EGTA, 10; ATP, 4; $MgCl_2$, 5; and imidazole, 20. The rigor solution contained K-propionate, 120; EGTA, 5; EDTA, 5; and imidazole, 20, with or without 20 mM BDM. For preservation purposes, 0.2 mM NaN_3 and 2.5 μg/ml of antipain (Sigma-Aldrich, St. Louis, MO) were added to the rigor solution. The photolysis solution contained K-propionate, 60; EGTA, 10; P^3-[1-(2-nitrophenyl)ethyl] adenosine 5′-triphosphate (NPE-caged ATP; Dojin, Kumamoto, Japan), 10; $MgCl_2$, 7.5; glutathione, 20; and imidazole, 60. The photolysis solution contained either 10.5 units/ml of apyrase (A 6535; Sigma-Aldrich) or a combination of 50 μM ADP and 250 μM diadenosine pentaphosphate (Sigma-Aldrich). The pH of all solutions was adjusted to 7.2. The temperature inside the specimen chamber was 4°C as determined by inserting a hypodermic thermocouple.

Photolysis

The specimen chamber was basically the same as described (Iwamoto et al., 2001), but it had a third quartz window to let in the UV-laser flash (Fig. 1 *A*). The laser beam had a round profile (diameter, ~7 mm) so that its width was reduced to 3 mm in the horizontal direction by using a cylindrical quartz lens to fit to the window. The beam size remained 7 mm in the vertical direction (along the fiber axis), so that the entire lengths of the fibers were illuminated. The fibers were flashed while they were in the caged ATP solution. The path length for the laser flash between the quartz window and the fiber was 0.5 mm. The UV laser flash (λ = 355 nm) was generated by a Nd-YAG

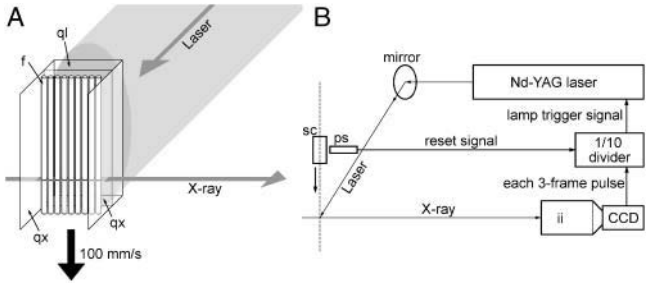

FIGURE 1 Experimental setup. (*A*) Specimen chamber. It had two thin quartz windows (*qx*) to let in and out the x-ray beams and a thick quartz window (*ql*) to let in the laser beams. (*f*) Single muscle fiber. The entire chamber was made to move vertically at a speed of 100 mm/s, and the picture is drawn so that the chamber is at the position at which the laser is flashed. (*B*) The construction of the entire system. (*sc*) Specimen chamber; (*ps*) photosensor; (*ii*) image intensifier; (*CCD*) CCD detector. For detailed explanations see Materials and Methods.

pulse laser (Surelite II-10, Continuum, Santa Clara, CA). The energy of each flash was 130 mJ and was sufficient to photolyze 20% of the caged ATP in the chamber.

X-ray diffraction

The x-ray diffraction experiments were performed at the BL40XU beamline of SPring-8 (''high-flux'' beamline; Inoue et al., 2001; Yagi, 2003). This beamline has a helical undulator capable of emitting quasimonochromatic x-rays without a monochromator. The total flux is $\sim 10^{15}$ photons/s, i.e., $\sim 10^3$ times higher than that of other undulator-based beamlines equipped with monochromators. At the center of the beam, its energy spectrum consists almost exclusively of fundamental waves. If only the central part of the beam is sliced out, its energy resolution ($\Delta E/E$) is 2%. Here a larger part of the beam was used to gain extra flux, and the energy resolution was ~3%. Nevertheless, the reflections in question were well resolved at this energy resolution. The energy of the x-ray beam was 15 keV ($\lambda = 0.083$ nm). The size of the beam at the sample was ~40 μm (vertical) $\times$ 250 μm (horizontal) (full width at half maximum). The camera length was 3 m in most cases, but for recordings of higher angle reflections, a camera length of 2.4 m was used.

The detector was a custom-made CCD camera (C7770, Hamamatsu Photonics, Hamamatsu, Japan) in combination with an image intensifier (V5445P, Hamamatsu Photonics). This CCD camera had three identical CCD chips (640 $\times$ 480 pixels), which were exposed alternately to achieve a frame rate of 3.4 ms/frame (Yagi, 2003).

Timing control of flash and recording

To minimize radiation damage, the specimen chamber was moved along the fiber axis at a constant speed of 100 mm/s by using a pulse-motor driven *z*-stage (Sigma-koki, Hidaka, Japan). Because of this movement, the total photons absorbed by the specimen were reduced to a level comparable to that in the BL45XU beamline, which has a flux of $\sim 10^{12}$ photons/s (for calculations see Appendix A). Since the fibers were ~6 mm long, it assured a ~60-ms duration of recording time including a brief preflash period. The three independently running components (the *z*-stage, the CCD camera, and the Nd-YAG laser, whose lamp must be continually triggered at 10 Hz) had to be synchronized to ensure that the laser was flashed at a fixed timing with respect to the CCD frames when the leading end of the specimen chamber was on the beam. To meet this demand, the three components were interconnected as in a manner shown in Fig. 1 *B*. The CCD camera continually generated a pulse in every three frames at an interval of 3.4 $\times$ 3 = 10.2 ms. The pulses were then divided by 10 by a digital counter to generate pulses to trigger the lamp of the Nd-YAG laser. The movement of the *z*-stage was started manually. At the moment when the moving stage passed by a photosensor placed a fixed distance ahead of the x-ray beam, it generated a pulse that initiated a recording sequence in the CCD camera and reset the digital counter. The whole system ensured that the Nd-YAG laser was flashed with an accuracy of 10.2 ms or 1.02 mm of the *z*-stage movement at the speed of 100 mm/s.

Data analysis

For each time frame, the two-dimensional diffraction patterns from a number of specimens were summed up, and the counts in the four quadrants were averaged to obtain an adequate signal/noise ratio before the patterns were subjected to background subtraction and profile analysis. The background subtraction and the intensity integration were done as described (Iwamoto et al., 2002, 2003a). The data processing was basically done by using software built in-house. Curve fittings for the time course of intensity changes and statistical analyses were done by using a commercial software package (Prism, Graphpad Software, San Diego, CA).

RESULTS

Overstretched muscle fibers with S1

This system is suitable for pursuing any transient structural changes that may occur in the actomyosin complex after ATP binding but before dissociation. Actomyosin complexes with a conformation distinct from that of rigor or with disordered configurations would be detected if they are significantly populated. This system is also free of sarcomeric disorder that might be generated by active force development.

Fig. 2 shows the selected frames of the time series of diffraction patterns taken before and after photolysis of caged ATP in overstretched fibers with S1. The pattern before photolysis (time $\leq$ 0) shows features of actin filaments fully decorated with S1 as have been well documented (e.g., Iwamoto et al., 2001, 2002): All the ALL's between the 1st and 7th are strongly enhanced, and the peak of the 6th ALL (at 1/5.9 nm^{-1}) is shifted toward the meridian. After photolysis, these ALL's faded off, leaving the much weaker 6th and 7th ALL's at the final stage of relaxation (the last pattern of the series in Fig. 2).

The intensity of each ALL was integrated in the area indicated by a box shown in the first pattern in Fig. 2. The 6th ALL has two boxes: One (inner part) is in the region where the intensity is most sensitive to stereospecifically attached S1, and the other (outer part), the least sensitive, but it is long known that the 6th ALL is enhanced as a whole during normal contraction or in the presence of Ca^{2+} (Parry and Squire, 1973; Matsubara et al., 1984; Kress et al., 1986; Wakabayashi et al., 1985, 1988; Maeda et al., 1988; Kraft et al., 1999; Iwamoto et al., 2003a).

The time courses of decay of these ALL's are shown in Fig. 3, either in the absence (Fig. 3 *A*) or presence (Fig. 3 *B*) of 50 μM ADP. The decay of the lower order ALL's (up to the 5th) and the inner part of the 6th ALL was fast (the decay was almost complete in ~30 ms at 0°C) and was adequately fitted by a single exponential decay function. The rate constants for these ALL's were all similar (Fig. 4). These are the ALL's whose intensities originate exclusively from stereospecifically attached S1. Inclusion of 50 μM ADP resulted in only a small tendency to slow the decay, and the differences were statistically insignificant. On the other hand, the 7th ALL and the outer part of the 6th ALL behaved differently. Their decay was slower and poorly fitted by a single exponential function (this is not merely because of lower counting statistics, but the behavior of reflections seems to be qualitatively different). These are the ALL's that have substantial intensities under relaxing conditions because actin contributes substantially to their intensities. It is obvious visually that the inclusion of 50 μM ADP had a greater slowing effect on the decay of these ALL's.

The changes of the intensity profiles of representative ALL's after photolysis, measured along the layer line, are shown in Fig. 5. It seems that the intensities of these ALL's,

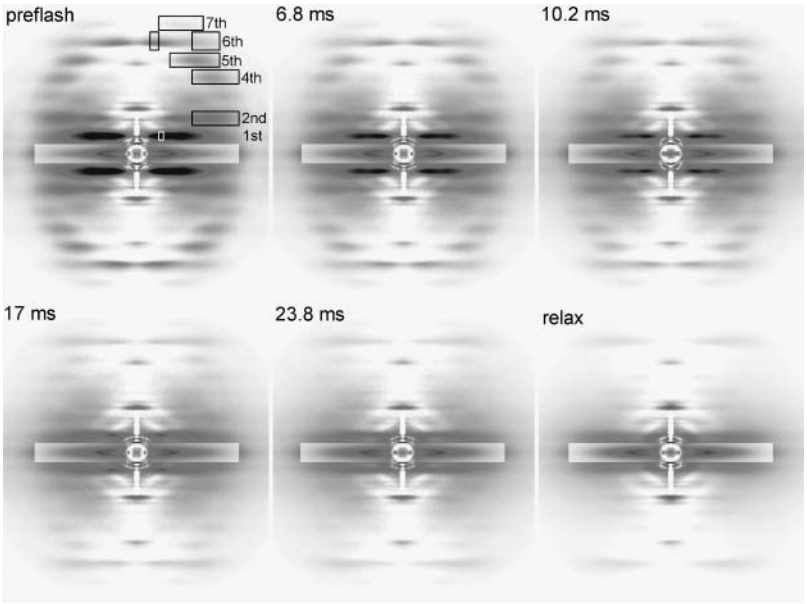

FIGURE 2 Selected frames of the time series of background-subtracted diffraction patterns taken during a caged ATP photolysis experiment using overstretched fibers with diffused S1. The four quadrants of each pattern have been averaged. The number in each pattern shows the time after flash. Recorded with a long (3 m) camera, in the absence of ADP. The boxes in the first (*preflash*) pattern show the areas of intensity integration (the *number* by the *box* indicates the order of the ALL). The patterns of the same time frame were summed for four independent beam times (25 sets of 30 single fibers).

to which stereospecifically attached S1 has major contributions, decreased without a change in their profiles. The centroids of these ALL's (shown as dots in the profiles) stayed almost in the same position during the decay until the intensities became very low.

The decrease of intensities without changing their profiles, along with similar rate constants for all the ALL's, is best explained if the S1 simply dissociates from actin without changing its configuration, although other possibilities are not excluded (see Discussion for details).

Fibers with full filament overlap

In this system, the configurations of myosin heads are influenced by the geometrical factors imposed by the other head of the same molecule and/or the thick filament backbone, and the thin filaments are occupied by the heads to a lesser extent than in the previous system. However, the experimental conditions are equivalent to those of mechanics measurements, and the results of the two types of measurements may be directly compared with each other.

Fig. 6 shows the selected frames of the time series of diffraction patterns taken before and after photolysis of caged ATP in fibers with full filament overlap, either in the presence or absence of 50 μM ADP. Although weaker than in the overstretched fibers, the ALL's were all enhanced in rigor, and they faded off after photolysis, leaving the 6th and 7th ALL's. In addition to the ALL's observed in the overstretched fibers, layer lines are observed at spacings of 23 nm and 10.4 nm. These layer lines arise because there are not enough myosin heads to decorate all the actin monomers, and the pattern of decoration is modulated by the myosin repeat on the thick filament (Yagi, 1996). These reflections were also weakened after photolysis.

The time courses of decay of the ALL's in the full-overlap fibers are shown in Fig. 7, either in the absence (Fig. 7 *A*) or presence (Fig. 7 *B*) of 50 μM ADP. Also superposed are the intensity of the 1,1 equatorial reflection and the separately

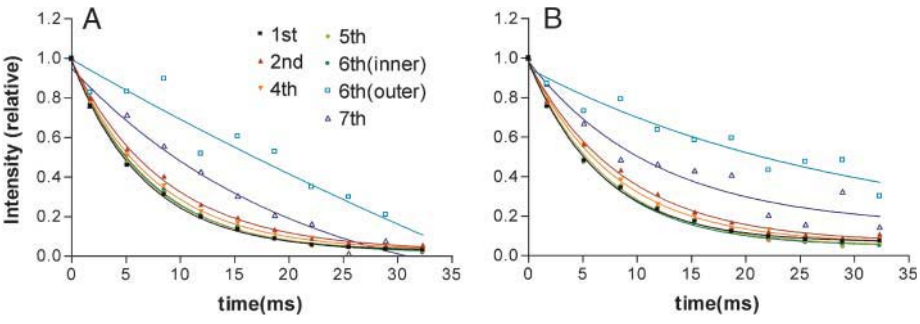

FIGURE 3 Time course of decay of the integrated intensities of ALL's after photolysis in overstretched fibers with diffused S1. (*A*) In the absence of ADP; (*B*) in the presence of 50 μM ADP. The intensities are normalized to the difference between the preflash and relaxed levels. Note that the time courses of decay of most of the ALL's (except for the *7th* and the *outer* part of the *6th*) are superposable to each other and well fitted by a single exponential decay (*curves*). The fitting was made to the same summed data as in Fig. 2, from four independent beam times (25 sets of 30 single fibers).

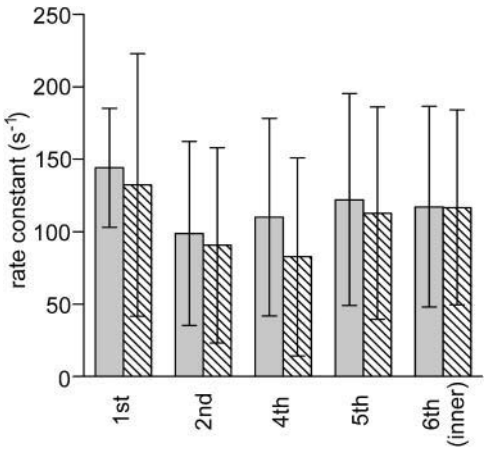

FIGURE 4 Summary of the rate constants for the decay of ALL's after photolysis in overstretched fibers with diffused S1. Each column represents the mean of the rate constants individually determined for different beam times (mean ± SE, $n = 4$). (*Shaded columns*) In the absence of ADP; (*hatched columns*) in the presence of 50 μM ADP. The data for the 7th and the outer part of the 6th ALL's are not shown because of the poor fit to a single exponential decay function.

recorded time course of tension decay. Both were highly dependent on ADP (for ADP effect on tension, see Dantzig et al., 1991; Thirlwell et al., 1994; for ADP effect on equatorial reflections, see Poole et al., 1991; Horiuti et al., 1994). Again, the decay of most of the ALL's (the ALL's whose intensities are exclusively attributed to stereospecifically attached myosin heads) was fast (faster than the tension decay) and adequately described by a single exponential function. The effect of ADP on the rate constants was generally greater than in the overstretched fibers and was statistically significant (Fig. 8 *A*). However, the ADP effect on the ALL's is still modest when compared with that on tension. The time course of the equatorial (1,1) reflection followed that of tension more closely, reflecting the fact that this reflection is also sensitive to nonstereospecific attachment of myosin heads to actin. The ALL's unique to fibers with filament overlap (at 23 nm and 10.4 nm) behaved similarly, but the decay of the ALL at 10.4 nm tended to be slower than the others, and some intensity remained after the other ALL's had dropped to zero, as is evident from the magnitude of the residual (time-independent) component (Fig. 8 *B*).

The decay of the 7th and 6th (outer part) ALL's was again slower and more dependent on ADP than in the rest of the ALL's and was poorly fitted by a single exponential function. In a separate measurement using a shorter camera, the time courses of decay were recorded for the ALL's including the outer part of the 2nd ALL (so-called tropomyosin reflection; *red symbols* and *curves* in Fig. 7). The decay of the outer part of the 2nd ALL was slow, and again its rate of decay was sensitive to ADP. Those ALL's to which the thin filament structure has major contributions (7th and the outer parts of the 2nd and 6th) seemed to behave similarly and more correlated with the time course of tension decay than other ALL's.

DISCUSSION

In this study, we recorded two-dimensional diffraction patterns from rabbit skinned skeletal muscle fibers relaxing from rigor after photolysis of caged ATP with a time resolution of 3.4 ms. The fibers were either overstretched and with exogenous rabbit skeletal muscle S1, or at full filament overlap without exogenous S1. With this time resolution, we were able to record the intensity changes of many actin-based reflections, which are much weaker than the more intense reflections previously measured in time-resolved caged-ATP experiments.

Structural changes of actomyosin complex upon ATP binding

The results using the system of overstretched fibers with exogenous S1 can be directly compared with expectations from the docked models of actin filaments decorated with S1 in rigor (for calculated ALL intensities, see e.g., Iwamoto et al., 2001). The earliest model (Moore et al., 1970) was refined in later studies (Rayment et al., 1993a; Lorenz et al., 1993) by including the atomic coordinates of actin (Kabsch et al., 1990) and S1 (Rayment et al., 1993b), and they reasonably reproduce the intensity profiles of ALL's as are presented here. The rigid spatial relationship between actin and S1 is presumably assured by the three-dimensional complementarity at the interface. It is unknown how this complementarity is destroyed upon ATP binding, but a nucleotide-driven interdomain movement may be implicated in the process (Volkmann et al., 2000).

As for the transient events that the ATP-bound actomyosin complex might experience before it eventually dissociates, we consider the following three possibilities that are experimentally testable by means of x-ray diffraction.

The first possibility is that, although the binding is weakened, the S1 remains bound stereospecifically for a brief period of time with a conformation distinct from that of the rigor complex (e.g., with a different orientation of the light chain binding domain). If this happens, the complex should give rise to a diffraction pattern similar to that of rigor, but the intensity profiles of ALL's should be different.

The second possibility is that the complex remains bound for a brief period, not in a stereospecific form any more but in a disordered state similar to the one found in the cross-linked actomyosin complex in the presence of ATP (Iwamoto et al., 2001). The consequence of this would be that the higher order ALL's are weakened more than the lower order ALL's (see the model calculations by Iwamoto et al., 2001). In the time series, such a mode of interaction is expected to have an effect that the higher order ALL's decay faster than the lower order ALL's after photolysis.

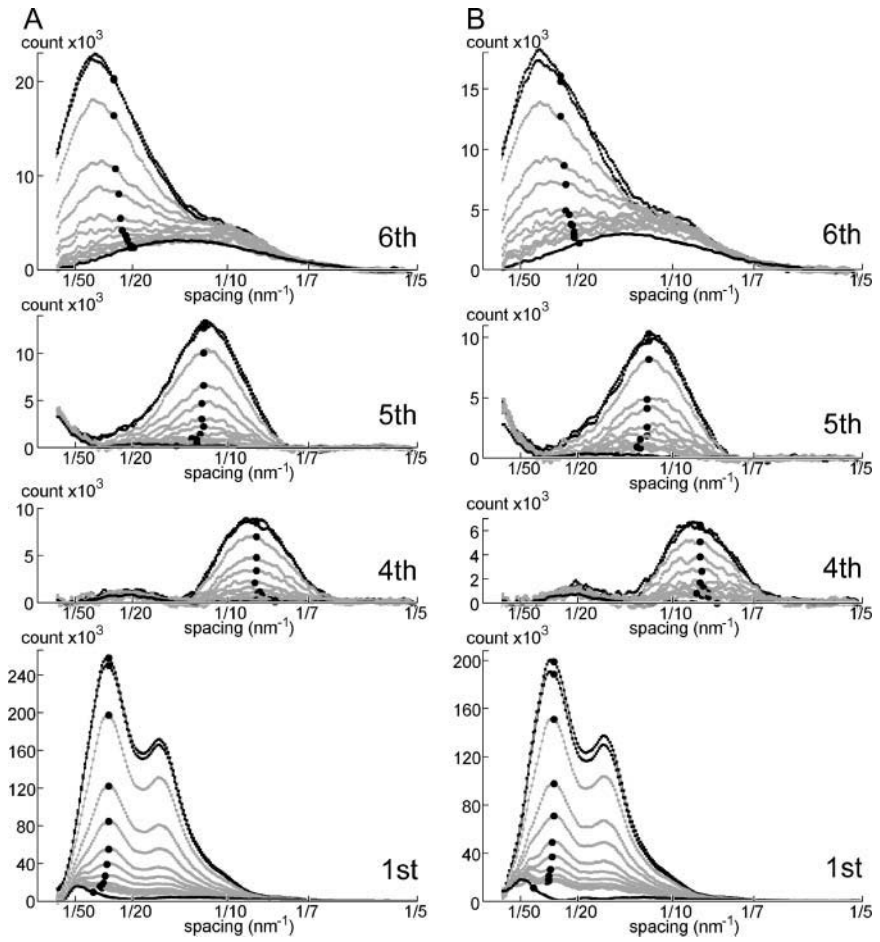

FIGURE 5 Intensity profiles of the representative ALL's before and after photolysis in overstretched fibers with diffused S1. (*A*) In the absence of ADP; (*B*) in the presence of 50 μM ADP. Taken from the summed patterns as shown in Fig. 2. The uppermost two solid curves in each set of profiles represent the preflash level, and the lowermost solid curve represents the relaxed level. The ● show the position of the centroids, calculated in the ranges between 1/60 nm^{-1} and 1/14 nm^{-1} for the 6th, between 1/50 nm^{-1} and 1/8 nm^{-1} for the 5th, between 1/12 nm^{-1} and 1/6.5 nm^{-1} for the 4th, and between 1/60 nm^{-1} and 1/18 nm^{-1} for the 1st ALL's (the peaks of the *1st* ALL may be affected by the lattice sampling). Note that the centroid positions do not move along the layer line until the intensities become very low.

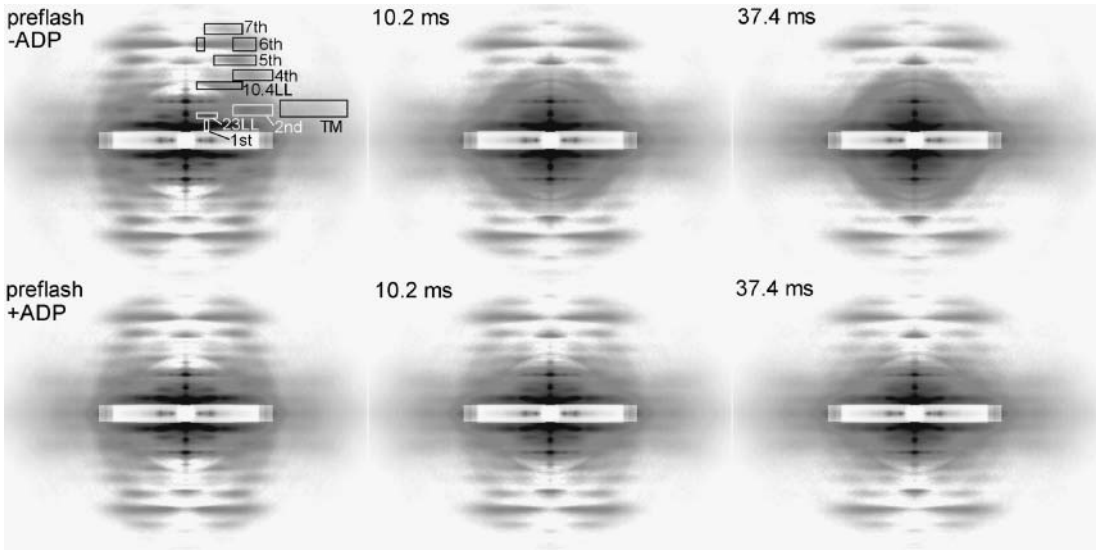

FIGURE 6 Selected frames of the time series of background-subtracted diffraction patterns taken during caged ATP photolysis experiment using fibers with full filament overlap. The upper and lower rows show the pattern recorded in the absence and presence of 50 μM ADP, respectively. The number in each pattern shows the time after flash. The patterns shown here are recorded in a single beam time in which a short (2.4 m) camera was used (nine or 10 sets of 30 single fibers). The boxes show the areas of intensity integration (the *number* by the *box* indicates the order of the ALL); 10.4LL and 23LL indicate the ALL's specific to fibers with filament overlap (spacings at 1/10.4 nm^{-1} and 1/23 nm^{-1}, respectively; see Yagi, 1996). TM indicates the outer part of the 2nd ALL (so-called tropomyosin layer line). Note that, in the presence of ADP, the outer part of the 2nd ALL is more clearly observed in the last frame.

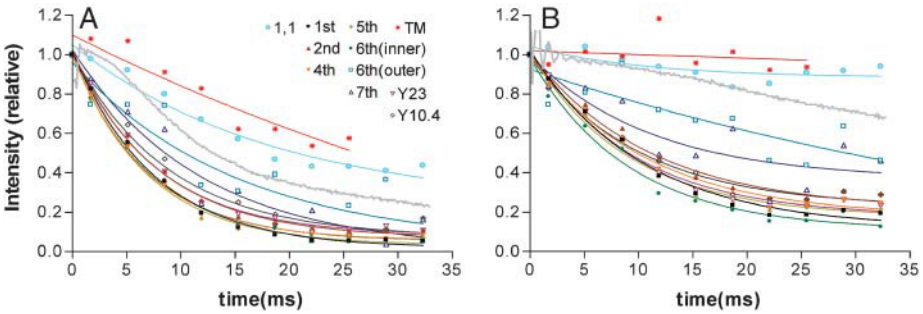

FIGURE 7 Time course of decay of the integrated intensities of ALL's and the 1,1 equatorial reflection after photolysis in fibers with full filament overlap. (*A*) In the absence of ADP; (*B*) in the presence of 50 μM ADP. The intensities are normalized to the difference between the preflash and relaxed levels, as in Fig. 3. The data were fitted by a single exponential decay (*curves*). The fitting was made to the data summed for five independent beam times (51 and 50 sets of 30 single fibers for the absence and presence of ADP, respectively), except for the data of the outer part of the 2nd ALL (*TM*), which were from a single beam time in which a short camera was used (see Fig. 6). The shaded curves are the tension recorded in a separate experiment done under conditions identical to those in x-ray diffraction experiments; 10.4LL and 23LL indicate the ALL's specific to fibers with filament overlap (spacings at 1/10.4 nm^{-1} and 1/23 nm^{-1}, respectively). The intensity of the equatorial 1,0 reflection was not accurately determined because of the size of the beamstop.

The third possibility is that the S1 molecules simply detach from actin without passing through any intermediate structure. In this case, it is expected that the intensity profiles of all the ALL's stay unchanged, and that the total intensities decrease proportionally. Thus, the time course of intensity decay should be the same for all the ALL's.

The results showed that the intensities of the ALL's decreased with similar rate constants without changes in their profiles. Thus the results are consistent with the last possibility, i.e., the actomyosin complex dissociates without passing though a state structurally distinct from rigor, although these results do not rule out the possibility of more subtle structural changes. If, for example, the structural change is confined to the actin-myosin interface, then it may affect only higher angle reflections that cannot be detected with this experimental system. Alternatively, a structural state distinct from rigor may exist, but this state may be too short-lived to be detected.

Rate of dissociation of actomyosin complex upon ATP binding

When the active component is minimized by including apyrase in the photolysis solution, the tension of skinned muscle fibers has been shown to decay with a time course expected from the rate constants for caged ATP photolysis and the second-order rate constant for the dissociation of the actomyosin complex (Martin and Barsotti, 1994). The rate constant for the dissociation of actomyosin upon ATP binding has been reported to be $\sim 10^6$ $M^{-1}s^{-1}$ at 5°C (Ma and Taylor, 1994; this should give an apparent first-order rate constant of 1000 s^{-1} at 1 mM ATP) and that for ATP photorelease is 118 s^{-1} at 20°C (Goldman et al., 1984a). With this combination of rate constants (relatively slow ATP release), it is expected that the dissociation of the rigor actomyosin complex starts slowly and then accelerates (see Appendix B). The slow start of dissociation is inevitable regardless of the magnitude of the rate constant for dissociation. In this context, it is worth noting that the decay of integrated intensities of the ALL's is almost perfectly fitted by a single exponential decay function, and no delay is observed (Fig. 3). A similar observation has been made for the equatorial reflections by Poole et al. (1991), who showed that the 1,1 equatorial reflection dropped with a half time of 3–4 ms after flash at 10–12°C. Similarly, the fast decay of the equatorial and the 1st ALL has been observed by Horiuti et al. (1997). As will be shown in Appendix B, the lack of the delay is evidence that caged ATP binds competitively to the active site of myosin and is photolyzed although remaining bound.

Although the perfect fit of this data to a single exponential decay is remarkable, extracting the second-order rate constant for the ATP binding to myosin is not straightforward. This is because the rate of myosin dissociation is much affected by the kinetics of caged ATP binding (see Appendix B). In addition, there is an unsettled issue as to how the number of diffracting units is related to reflection intensities. It is generally understood that the intensity of the x-ray reflection is proportional to the square of the number of diffracting units (square law; e.g., Haselgrove, 1975). Recently, however, Tsaturyan (2002) and Koubassova and Tsaturyan (2002) showed that a significant deviation from the square law may arise if the binding pattern of S1 is not random (this is especially true for fibers with full filament overlap, in which the myosin binding pattern is modulated by the 14.5-nm repeat on the thick filament). An independent study shows that the relation between the amount of S1 in overstretched fibers and reflection intensities can be anywhere between a linear relationship and the one described by the square law, depending of the pattern of S1 binding on actin (Tamura et al., 2004).

ADP effect on the transient active contraction

The system using fibers with full filament overlap is suitable for studying how the ATP-induced dissociation process of

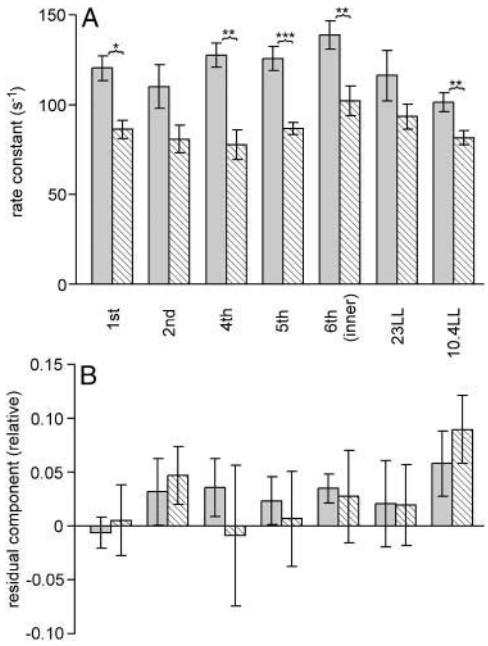

FIGURE 8 Summary of the analysis of the decay of ALL's after photolysis in fibers with full filament overlap. (*A*) Rate constants. (*Shaded columns*) In the absence of ADP; (*hatched columns*) in the presence of 50 μM ADP (mean ± SE, $n = 5\sim6$). The asterisks indicate that there is a statistically significant difference between the data in the absence and those in the presence of 50 μM ADP (*, $p \leq 0.05$; **, $p \leq 0.01$; ***, $p \leq 0.001$). (*B*) Amount of the residual (time-independent) component remaining after the exponential decay is complete. Expressed relative to the difference between the preflash and relaxed levels of integrated intensities (the same scale as in Fig. 7). Note that the residual component is exceptionally large for the ALL at 1/10.4 nm^{-1}. Each column shows the mean of the rate constants individually determined for different beam times (mean ± SE, $n = 5\sim6$). The data for some of the ALL's are not shown because of the poor fit to a single exponential decay function.

actomyosin affects the thin filament regulatory system and, in turn, the activity of myosin heads. Importantly, this system allows direct comparisons between reflection intensities and our and earlier (Goldman et al., 1982, 1984a; Thirlwell et al., 1994) mechanical measurements. Goldman et al. (1984a) considered the rise of the out-of-phase stiffness as evidence that, during relaxation after photolysis, some myosin heads had properties similar to those in calcium-activated normal contraction. However, the presence of the out-of-phase stiffness per se is not sufficient to prove that these myosin heads are identical to those in actively contracting muscle. Moreover, Horiuti and Kagawa (1998) proposed that the initial phase of the active force is generated by a different mechanism, i.e., a force generation coupled to the transition from A·M to A·M·ATP forms (A and M stand for actin and myosin, respectively). What information can the x-ray results provide to further characterize the myosin heads during the active phase of photolysis-induced relaxation?

It is known that the myosin heads actively cycling during calcium-activated normal contraction contribute little to the ALL's that would be enhanced in rigor (Huxley and Brown, 1967; Wakabayashi et al., 1988; Iwamoto et al., 2003a), suggesting that the force-generating myosin heads are nonstereospecifically attached to actin during contraction. In the photolysis experiments, the intensities of those ALL's decreased promptly, whereas in the presence of ADP, tension was maintained long after their intensities had decreased to a very low level. Importantly, the equatorial reflection (1,1), which is sensitive to both stereospecific and nonstereospecific myosin binding, closely follows the tension change (Fig. 7). Thus, the force-supporting myosin heads in the later stage of photolysis-induced relaxation are also considered to be nonstereospecifically attached to actin and share the properties of the heads seen during calcium-activated normal contraction. In this context, it is worth noting that the layer line at 1/10.4 nm^{-1} decayed more slowly than other ALL's. This is the only ALL that has a noticeable intensity during normal contraction and whose intensity is exclusively derived from attached myosin heads (Iwamoto et al., 2003a). Therefore, the slower decay of this reflection is another indication of a similarity between the active phase of photolysis-induced relaxation and calcium-activated normal contraction, in support of the interpretation by Goldman et al. (1984a). We did not so far detect any sign of attached myosin heads whose properties were distinct from those of both rigor and normal actively cycling heads.

The period of active contraction seems to parallel the period of the thin filament activation. In Fig. 7, we have shown that the outer part of the 2nd ALL (so-called tropomyosin reflection) decayed slowly in a highly ADP-dependent manner. Traditionally, the enhancement of this reflection has been ascribed to the movement of the tropomyosin molecules on the thin filament to expose the myosin binding site on actin (Huxley, 1973; Parry and Squire, 1973). Recently, it has been suggested that factors other than tropomyosin also contribute to this reflection (see Squire and Morris, 1998; Iwamoto et al., 2002, and the references therein). Among others, the myosin contribution may be substantial in rigor, but this should fade off as other myosin-enhanced ALL's do. Thus, the intensity of the 2nd ALL remaining long after the photolysis should reflect the tropomyosin in the on position or other regulation-related structural changes of the thin filament.

Another indication for the thin filament involvement is the behavior of the 6th (outer part) and 7th ALL's. These ALL's decay more slowly than other ALL's and are sensitive to ADP. These reflections are the ALL's observable in the relaxed state and are substantially enhanced during contraction. Their enhancement during contraction has been difficult to explain in terms of myosin binding to actin, but is better explained in terms of structural changes of actin itself, rather than myosin attachment to actin (Iwamoto et al., 2003a, and the references therein). During relaxation of living muscles, the decay of these reflections (as well as the 2nd ALL) closely follows that of tension rather than intracellular

calcium (Iwamoto et al., 2003a), suggesting that the structural change of actin is induced by the binding of cycling myosin heads. This structural change may in turn enhance further myosin binding, thereby taking part in the thin filament regulation.

These considerations suggest that the tension during the active phase is not maintained by the initial stereospecific A·M or A·M·ADP complexes remaining after photolysis, but through a self-sustained mechanism involving an interplay between the actively cycling (reattached) myosin heads and the thin filament regulatory system. Why is the active phase prolonged in the presence of ADP? It is probably because another (nonstereospecific) A·M·ADP intermediate is generated during the normal ATPase cycle, and its population is increased in the presence of ADP. This intermediate is likely to be the major force-bearing species during contraction and is expected to be equally effective in keeping the thin filament regulatory system activated. This A·M·ADP intermediate has been suggested to be distinct from the one generated by the addition of ADP to rigor complexes (Sleep and Hutton, 1980). This view is supported by the caged chelator experiments using frog skinned muscle fibers, in which the concentration of calcium was suddenly reduced by the photolysis of diazo-2. The following relaxation was markedly slowed in the presence of a low (20 μM) concentration of ADP (Lipscomb et al., 1999). In contracting frog muscle, the amount of stereospecific actomyosin complexes is reported to be especially small (Iwamoto et al., 2003a), and it is unlikely that these complexes play any role in prolonging the relaxation of their specimens.

The effect of the two-headedness of myosin

In this study, both single-headed (S1) and two-headed (intact myosin) preparations were used. The dissociation of the actomyosin complex after caged ATP photolysis was slower and more ADP-sensitive in the two-headed preparation (the ADP effect was significant in the two-headed preparation but not in the single-headed preparation; see Figs. 4 and 8). Apart from the possible effect of proteolysis in preparing S1, this result suggests that there is cooperativity between the two heads of a myosin molecule, in support of the previous idea (Goldman et al., 1984a; Dantzig et al., 1991; Thirlwell et al., 1994). However, a distinction should be made between this cooperative effect and the effect of prolonging the active phase of relaxation, in which the thin filament regulatory system is implicated. One possible mechanism for the cooperativity would be that the dissociation step is reversible and there is a fast equilibrium between the associated and dissociated states: If one of the heads remains associated, it will keep the second head in the vicinity of actin, thereby increasing the effective concentration of actin. This will in turn slightly increase the probability of the second head to reassociate with actin in a stereospecific manner.

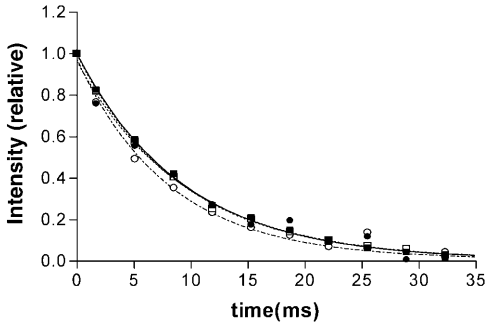

FIGURE 9 Time course of decay of the integrated intensities of major ALL's of fibers with full filament overlap, obtained from repeated flash experiments. After the first flash run, the fibers were placed in the rigor solution containing 20 mM BDM and then in the caged ATP solution for the second flash run. The caged ATP solution contained 50 μM ADP. The intensities are normalized to the difference between the preflash and relaxed levels, as in Fig. 3. Data from five sets of 30 single fibers were summed and fitted by a single exponential decay (*curves*). (*Squares*) The 1st ALL; (*circles*) the 5th ALL. (*Solid symbols*) Data obtained from the first flash run; (*open symbols*) the second flash run. Note that the curves for the first and second flashes are almost superposable to each other. For the first flash, the rate constants of decay were 108 s^{-1} and 105 s^{-1} for the 1st and 5th ALL's, respectively. For the second flash, the rate constants were 109 s^{-1} and 123 s^{-1}, respectively.

APPENDIX A: ESTIMATION OF TOTAL X-RAY FLUX RECEIVED BY A UNIT LENGTH OF MUSCLE FIBERS

In the BL45XU beamline (a conventional undulator-based beamline equipped with a monochromator), muscle fiber specimens as used here are known to withstand at least 3 s exposure without appreciable radiation damage. In this beamline, the dimension of the x-ray beam is typically 400 μm (vertical) $\times$ 600 μm (horizontal) (full width at half maximum) with a flux of 10^{12} photons/s. We assume that the width of the fiber is 100 μm and for simplicity do not take the beam profile into consideration, and the total flux received by a 1-mm segment of specimen is calculated to be 1.25 $\times$ 10^{12} photons/mm (= 10^{12} $\times$ 100/600/0.4 $\times$ 3).

In the case of the high-flux BL40XU beamline, the dimension of the beam is typically 40 μm (vertical) $\times$ 250 μm (horizontal), and the flux is 10^{15} photons/s. Let w be the vertical width of the beam (mm), with the speed of the z axis stage being 100 mm/s; the total flux received by a 1-mm segment of the specimen is calculated to be 4 $\times$ 10^{12} photons/mm (= 10^{15} $\times$ 100/250/w $\times$ w/100). It is clear from this calculation that the total flux received does not depend on the extent of vertical beam focusing.

The energies of the x-ray beams were 12.4 keV and 15 keV for BL45XU and BL40XU, respectively, and at these energies, the attenuation lengths of water (length of materials that reduces the flux to 1/e) are 3789.40 μm and 6631.42 μm, respectively (obtained from the Center for X-Ray Optics at the web site http://www-cxro.lbl.gov/). This means that the photons absorbed by the materials at 15 keV are about half that at 12 keV for a given x-ray flux.

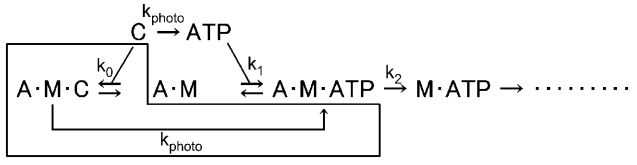

SCHEME 1

Thus, the numbers of photons absorbed by the material (i.e., the measure of radiation damage) are considered comparable in these two beamlines. In addition, we should point out here that radiation damage, if any, would little affect the time course of S1 dissociation. This is because, due to the fast stage movement, different parts of the specimen receive x-ray radiation for the first time after different amounts of S1 have already dissociated.

Fig. 9 shows the effect of repeated x-ray exposures on the time courses of decay of the ALL's in the full-overlap fibers. After the first photolysis run, the fibers were placed in the rigor solution and then subjected to a second photolysis run. The speed of the *z*-stage movement was 50 mm/s, so that the fibers received twice as much flux as in the rest of the experiments. Despite this higher dose, the time courses of decay in the second run remain unchanged. This demonstrates that the damage caused by the first exposure to x-ray is negligible, especially when the specimen is moved at 100 mm/s.

APPENDIX B: CALCULATED TIME COURSE OF ACTOMYOSIN DISSOCIATION AFTER PHOTOLYSIS OF CAGED ATP

In general, the purpose of the use of caged compounds to biological systems is to study enzymatic reactions in the cell that are too fast to study by diffusing biologically active compounds from the outside. Caged ATP was introduced to the field of muscle study for the same reason (Goldman et al., 1982, 1984a,b). However, the most commonly used form of caged ATP (NPE-caged ATP) is known to have two drawbacks: One is that the liberation of ATP after photon absorption (dark reaction) is slow (Goldman et al., 1984a), and the other is that it acts as a competitive inhibitor of ATP if not photolyzed (Sleep et al., 1994; Thirlwell et al., 1995) (the latter also applies to the fast-photolyzing P3-3′,5′-dimethoxybenzoin ester of ATP (DMB-caged ATP); Thirlwell et al., 1995). To evaluate the effect of these properties, the time course of actomyosin dissociation (and therefore that of the decay of ALL intensities) are calculated here by an iterative procedure.

Two cases are considered. In case I, it is assumed that photoreleased ATP is initially free in solution and binds to the myosin nucleotide binding site through a diffusion process. In case II, the competitive binding of caged ATP to the myosin nucleotide binding site is taken into consideration. The bound caged ATP is allowed to photolyze with the same rate constant as for free caged ATP. The calculations are based on the following reaction scheme where A, M, and C stand for actin, myosin, and caged ATP, respectively. In case I, the part of the scheme in the box is not considered. The binding constants of ATP and caged ATP for myosin are assumed to be 10^{11} M^{-1} and 10^{3} M^{-1}, respectively (see Sleep et al., 1994; Thirlwell et al., 1994). The value of $k_1{}^{+}$ is assumed to be 10^{6} $M^{-1}s^{-1}$ (at 5°C; Ma and Taylor, 1994). The initial concentration of caged ATP is 10 mM, and 2 mM of ATP is assumed to be photoreleased. The rate of release of ATP (k_{photo}) is ~120 s^{-1} at 20°C, and if its activation enthalpy is taken into consideration, it would be ~40 s^{-1} at 4°C (Barabas and Keszthelyi, 1984). However, values greater than this yield more realistic rate constants for actomyosin dissociation.

Fig. 10 *A* shows the case without competitive binding (case I), with a k_{photo} value of 80 s^{-1}. The entire dissociation process (thus the decay of x-ray intensities) is poorly fitted by a single exponential function regardless of the choice of rate constants. The initial delay of dissociation is always evident, because ATP starts with low concentrations. The best-fit rate constants for the decay of x-ray intensities are 84 s^{-1} and 127 s^{-1} for the linear relationship and the square law, respectively.

On the other hand, it is remarkable that the delay seen in case I is virtually eliminated by assuming the preflash binding of caged ATP and its photolysis while bound to myosin (Fig. 10 *B*), provided the binding kinetics of caged ATP from S1 is slow relative to k_{photo}. In Fig. 10 *B*, The value of $k_0{}^{-}$ is 8×10^{4} $M^{-1}s^{-1}$ and other constants are the same as in Fig. 10 *A*. Now the entire time course of dissociation is far better fitted to a single exponential function, whether the square law or the linear law applies. The best-fit rate constants for the decay of x-ray intensities are 53 s^{-1} and 98 s^{-1} for the linear relationship and the square law, respectively, and the values are affected much by the choice of $k_0{}^{-}$. The accelerating effect of the preflash caged ATP binding in the initial part of the dissociation is evident from the comparison of time courses in the first 10 ms after photolysis for cases I and II (*inset* in Fig. 10 *B*), and becomes more evident as a greater percentage of caged ATP is photolyzed.

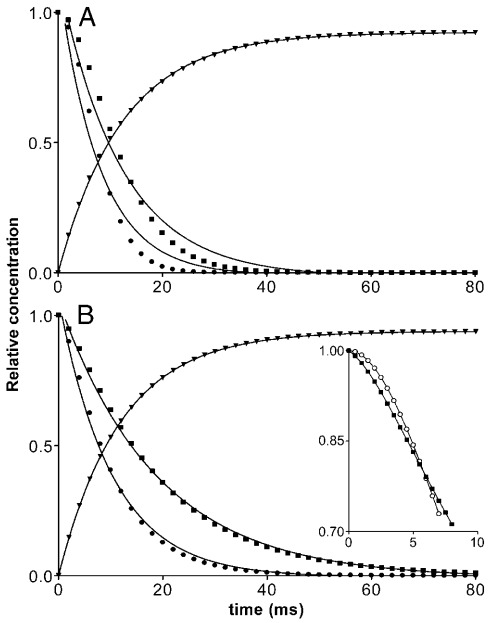

FIGURE 10 Calculated time course of change of rigor complex concentration, based on the scheme in Appendix B. In both cases, it is assumed that the rate constant for ATP release is 80 s^{-1}, 2 mM out of 10 mM caged ATP is photolyzed and the rate constant $k_1{}^{+}$ is 10^{6} $M^{-1}s^{-1}$. The reverse rate constant $k_1{}^{-}$ is set so as to satisfy the ATP binding constant (10^{11} M^{-1}). The concentration of myosin head is assumed to be 0.15 mM. The diffusion of photoreleased ATP from the surrounding medium is not considered. (*A*) Case I, in which caged ATP binding to myosin is not taken into consideration. (■) Relative concentration of the rigor complexes (this is also the time course of decay of ALL intensities if they are linearly related to the amount of the rigor complex); (●) rigor complex concentration squared (this is the time course of decay of ALL intensities if they obey the square law); (▼) concentration of liberated ATP, fitted by a single exponential association function (*curve*). Note the delay in the rigor complex dissociation. The simulated data are poorly fitted by a single exponential decay function (*curves*). Other rate constants: $k_2{}^{+}$, 10^{4} s^{-1}, $k_2{}^{-}$, 0 s^{-1}. (*B*) Case II, in which caged ATP is assumed to bind to myosin and is photolyzed on the spot upon flash. Note that the initial delay seen in *A* has disappeared. The rate constant $k_0{}^{-}$ is assumed to be 8×10^{4} $M^{-1}s^{-1}$. The time course of rigor complex dissociation and its square are well fitted by single exponential decay functions (*curves*). Symbols are the same as in A. The reverse rate constant for step 0 is set to meet the binding constant 10^{3} M^{-1}. The inset in *B* shows the superposition of the time courses of dissociation for case I (○) and case II (■). The delay of dissociation is reduced in case II, in which competitive binding of caged ATP is assumed.

Why does the competitive binding of caged ATP *accelerate* the initial part of dissociation? At a caged ATP concentration of 10 mM, >90% of the myosin is in the A·M·C form. Caged ATP acts as a competitive inhibitor, and this means that either it binds directly to the active site of myosin or it binds to a site close to the active site so that it effectively blocks the binding of ATP. Thus, as the caged ATP is photolyzed while it remains bound to S1, it can start to produce A·M·ATP complexes without being limited by the concentration-dependent diffusion process. Moreover, the preflash binding of caged ATP effectively increases the total content of caged ATP in the fiber. Although only 20% of the bound caged ATP may be photolyzed, it

will have no effect but to accelerate the dissociation. By the time when its initial accelerating effect fades off, the ATP concentration in the bathing medium will have increased to a substantial level, supporting the continuous dissociation of myosin heads by replacing the unphotolyzed bound caged ATP. Finally, all of the myosin heads will dissociate from actin, because the photogenerated ATP has a much (10^8 times) higher affinity for myosin and will replace all the bound caged ATP. The good agreement between the observed and calculated time courses suggests that case II, with relatively slow kinetics of caged ATP binding, represents the true mechanism of reaction.

The relation between the rate of myosin dissociation and the second-order rate constant for the binding of ATP is not straightforward, because the former is much influenced by the unknown rate constants for the association and dissociation of caged ATP to myosin. If the kinetics of caged ATP binding is slow (Fig. 10 *B*), the decay of the ALL intensities is well fitted by a single exponential decay function, whether the linear or the square law applies. However, the caged ATP dissociation tends to limit the rate of actomyosin dissociation, concealing the true actomyosin kinetics. If the kinetics of caged ATP binding is fast, the decay of the ALL intensities is accelerated, but it results in a poorer fit to a single exponential decay function (data not shown). Therefore, to correctly evaluate the actomyosin reaction kinetics from caged-ATP experiments, it is essential to determine the binding kinetics of caged ATP. This argument also applies to the fast-photolyzing P3-3′,5′-dimethoxybenzoin ester of ATP (Thirlwell et al., 1994; Tsaturyan et al., 1999), which has also been shown to bind competitively to myosin (Thirlwell et al., 1995).

We thank Drs. K. Inoue and T. Oka for their help at the beamline and Ms. R. Ryu for her technical assistance.

This work was performed under approval of the SPring-8 Proposal Review Committee (proposals 2001B0186-NL-np and 2002A0552-NL2-np) and supported by SPring-8 Joint Research Promotion Scheme of Japan Science and Technology Corporation and Special Coordination Funds of the Ministry of Education, Culture, Sports, Science and Technology, Japan.

REFERENCES

Barabas, K., and L. Keszthelyi. 1984. Temperature dependence of ATP release from ''caged'' ATP. *Acta Biochim. Biophys. Acad. Sci. Hung.* 19:305–309.

Dantzig, J. A., M. G. Hibberd, D. R. Trentham, and Y. E. Goldman. 1991. Cross-bridge kinetics in the presence of MgADP investigated by photolysis of caged ATP in rabbit psoas muscle fibres. *J. Physiol. (Lond.).* 432:639–680.

Goldman, Y. E., M. G. Hibberd, J. A. McCray, and D. R. Trentham. 1982. Relaxation of muscle fibres by photolysis of caged ATP. *Nature.* 300:701–705.

Goldman, Y. E., M. G. Hibberd, and D. R. Trentham. 1984a. Relaxation of rabbit psoas muscle fibres from rigor by photochemical generation of adenosine-5′-triphosphate. *J. Physiol. (Lond.).* 354:577–604.

Goldman, Y. E., M. G. Hibberd, and D. R. Trentham. 1984b. Initiation of active contraction by photogeneration of adenosine-5′-triphosphate in rabbit psoas muscle fibres. *J. Physiol. (Lond.).* 354:605–624.

Goody, R. S., K. Güth, Y. Maéda, K. J. V. Poole, and G. Rapp. 1985. Time-resolved X-ray diffraction measurements on *Lethocerus* fribrillar flight muscle following the photolytic release of ATP from 'caged-ATP.' *J. Physiol. (Lond.).* 364:75P.

Haselgrove, J. C. 1975. X-ray evidence for conformational changes in the myosin filaments of vertebrate striated muscle. *J. Mol. Biol.* 92: 113–143.

Horiuti, K., and K. Kagawa. 1998. Effects of ADP and low ATP on the Ca^{2+}-sensitive transient contraction upon photolysis of caged ATP in rat muscle fibres: a study on the Bremel-Weber type cooperation. *J. Muscle Res. Cell Motil.* 19:923–930.

Horiuti, K., N. Yagi, K. Kagawa, K. Wakabayashi, and K. Yamada. 1994. X-ray equatorial diffraction during ATP-induced Ca^{2+}-free muscle contraction and the effect of ADP. *J. Biochem. (Tokyo).* 115:953–957.

Horiuti, K., N. Yagi, and S. Takemori. 1997. Mechanical study of rat soleus muscle using caged ATP and X-ray diffraction: high ADP affinity of slow cross-bridges. *J. Physiol. (Lond.).* 502:433–447.

Horiuti, K., N. Yagi, and S. Takemori. 2001. Single turnover of cross-bridge ATPase in rat muscle fibers studies by photolysis of caged ATP. *J. Muscle Res. Cell Motil.* 22:101–109.

Huxley, H. E. 1973. Structural changes in the acitn- and myosin-containing filaments during contraction. *Cold Spring Harb. Symp. Quant. Biol.* 37:361–376.

Huxley, H. E., and W. Brown. 1967. The low-angle X-ray diagram of vertebrate striated muscle and its behaviour during contraction and rigor. *J. Mol. Biol.* 30:383–434.

Inoue, K., T. Oka, T. Suzuki, N. Yagi, K. Takeshita, S. Goto, and T. Ishikawa. 2001. Present status of high flux beamline (BL40XU) at SPring-8. *Nucl. Instr. Methods Phys. Res. A.* 467/8:674–677.

Iwamoto, H. 1995. Strain sensitivity and turnover rate of low force cross-bridges in contracting skeletal muscle fibers in the presence of phosphate. *Biophys. J.* 68:243–250.

Iwamoto, H., K. Oiwa, T. Suzuki, and T. Fujisawa. 2001. X-ray diffraction evidence for the lack of stereospecific protein interactions in highly activated actomyosin complex. *J. Mol. Biol.* 305:863–874.

Iwamoto, H., K. Oiwa, T. Suzuki, and T. Fujisawa. 2002. States of thin filament regulatory proteins as revealed by combined cross-linking/X-ray diffraction techniques. *J. Mol. Biol.* 317:707–720.

Iwamoto, H., J. Wakayama, T. Fujisawa, and N. Yagi. 2003a. Static and dynamic x-ray diffraction recordings from living mammalian and amphibian skeletal muscles. *Biophys. J.* 85:2492–2506.

Iwamoto, H., J. Wakayama, T. Tamura, T. Fujisawa, and N. Yagi. 2003b. X-ray evidence for structural changes of thin filament induced by cycling myosin heads. *Biophys. J.* 84:248a.

Kabsch, W., H. G. Mannherz, D. Suck, E. F. Pai, and K. C. Holmes. 1990. Atomic structure of the actin:DNase I complex. *Nature.* 347:37–44.

Kaplan, J. H., B. Forbush III, and J. F. Hoffman. 1978. Rapid photolytic release of adenosine 5′-triphosphate from a protected analogue: utilization by the Na:K pump of human red blood cell ghosts. *Biochemistry.* 17:1929–1935.

Koubassova, N. A., and A. K. Tsaturyan. 2002. Direct modeling of x-ray diffraction pattern from skeletal muscle in rigor. *Biophys. J.* 83:1082–1097.

Kraft, T., S. Xu, B. Brenner, and L. C. Yu. 1999. The effect of thin filament activation on the attachment of weak binding cross-bridges: a two-dimensional x-ray diffraction study on single muscle fibers. *Biophys. J.* 76:1494–1513.

Kress, M., H. E. Huxley, A. R. Faruqi, and J. Hendrix. 1986. Structural changes during activation of frog muscle by time-resolved X-ray diffraction. *J. Mol. Biol.* 188:325–342.

Lipscomb, S., R. E. Palmer, Q. Li, L. D. Allhouse, T. Miller, J. D. Potter, and C. C. Ashley. 1999. A diazo-2 study of relaxation mechanisms in frog and barnacle muscle fibres: effects of pH, MgADP, and inorganic phosphate. *Pflügers Arch.* 437:204–212.

Lorenz, M., D. Popp, and K. C. Holmes. 1993. Refinement of the F-actin model against X-ray fiber diffraction data by the use of a directed mutation algorithm. *J. Mol. Biol.* 234:826–836.

Ma, Y.-Z., and E. W. Taylor. 1994. Kinetic mechanism of myofibril ATPase. *Biophys. J.* 66:1542–1553.

Maeda, Y., D. Popp, and S. M. McLaughlin. 1988. Cause of changes in the thin filament-associated reflexions on activation of frog muscle-myosin binding or conformational change of actin. *Adv. Exp. Med. Biol.* 226:381–390.

Martin, H., and R. J. Barsotti. 1994. Relaxation from rigor of skinned trabeculae of the guinea pig induced by laser photolysis of caged ATP. *Biophys. J.* 66:1115–1128.

Matsubara, I., N. Yagi, H. Miura, M. Ozeki, and T. Izumi. 1984. Intensification of the 5.9-nm actin layer line in contracting muscle. *Nature*. 312:471–473.

Moore, P. B., H. E. Huxley, and D. J. DeRosier. 1970. Three-dimensional reconstruction of F-actin, thin filaments and decorated thin filaments. *J. Mol. Biol.* 50:279–295.

Parry, D. A. D., and J. M. Squire. 1973. Structural role of tropomyosin in muscle regulation: analysis of the X-ray diffraction patterns from relaxed and contracting muscles. *J. Mol. Biol.* 75:33–55.

Poole, K. J. V., Y. Maéda, G. Rapp, and R. S. Goody. 1991. Dynamic X-ray diffraction measurements following photolytic relaxation and activation of skinned rabbit psoas fibres. *Adv. Biophys.* 27:63–75.

Poole, K. J. V., G. Rapp, Y. Maéda, and R. S. Goody. 1988. The time course of changes in the equatorial diffraction patterns from different muscle types on photolysis of caged-ATP. *Adv. Exp. Med. Biol.* 226:391–404.

Rayment, I., H. M. Holden, M. Whittaker, C. B. Yohn, M. Lorenz, K. C. Holmes, and R. A. Milligan. 1993a. Structure of the actin-myosin complex and its implications for muscle contraction. *Science*. 261: 58–65.

Rayment, I., W. R. Rypniewski, B. Schmidt-Base, R. Smith, D. R. Tomchick, M. M. Benning, D. A. Winkelmann, G. Wesenberg, and H. M. Holden. 1993b. Three-dimensional structure of myosin subfragment-1: a molecular motor. *Science*. 261:50–58.

Sleep, J., C. Herrmann, T. Barman, and F. Travers. 1994. Inhibition of ATP binding to myofibrils and acto-myosin subfragment 1 by caged ATP. *Biochemistry*. 33:6038–6042.

Sleep, J. A., and R. L. Hutton. 1980. Exchange between inorganic phosphate and adenosine 5′-triphosphate in the medium by actomyosin subfragment 1. *Biochemistry*. 19:1276–1283.

Squire, J. M., and E. P. Morris. 1998. A new look at thin filament regulation in vertebrate skeletal muscle. *FASEB J.* 12:761–771.

Tamura, T., J. Wakayama, T. Fujisawa, N. Yagi, and H. Iwamoto. 2004. Intensity of X-ray reflections from skeletal muscle thin filaments partially occupied with myosin heads: effect of cooperative binding. *J. Muscle Res. Cell Motil.* In press.

Thirlwell, H., J. E. T. Corrie, G. P. Reid, D. R. Trentham, and M. A. Ferenczi. 1994. Kinetics of relaxation from rigor of permeabilized fast-twitch skeletal fibers from the rabbit using a novel caged ATP and apyrase. *Biophys. J.* 67:2436–2447.

Thirlwell, H., J. A. Sleep, and M. A. Ferenczi. 1995. Inhibition of unloaded shortening velocity in permeabilised muscle fibers by caged-ATP compounds. *J. Muscle Res. Cell Motil.* 16:131–137.

Tsaturyan, A. K. 2002. Diffraction by partially occupied helices. *Acta Crystallogr.* A58:292–294.

Tsaturyan, A. K., S. Y. Bershitsky, R. Burns, Z. H. He, and M. A. Ferenczi. 1999. Structural responses to the photolytic release of ATP in frog muscle fibres, observed by time-resolved X-ray diffraction. *J. Physiol. (Lond.).* 520:681–696.

Volkmann, N., D. Hanein, G. Ouyang, K. M. Trybus, D. J. DeRosier, and S. Lowey. 2000. Evidence for cleft closure in actomyosin upon ADP release. *Nat. Struct. Biol.* 7:1147–1155.

Wakabayashi, K., H. Tanaka, Y. Amemiya, A. Fujishima, T. Kobayashi, T. Hamanaka, H. Sugi, and T. Mitsui. 1985. Time-resolved X-ray diffraction studies on the intensity changes of the 5.9 and 5.1 nm actin layer lines from frog skeletal muscle during an isometric tetanus using synchrotron radiation. *Biophys. J.* 47:847–850.

Wakabayashi, K., Y. Ueno, Y. Amemiya, and H. Tanaka. 1988. Intensity changes of actin-based layer lines from frog skeletal muscles during an isometric contraction. *Adv. Exp. Med. Biol.* 226:353–367.

Yagi, N. 1996. Labelling of thin filaments by myosin heads in contracting and rigor vertebrate skeletal muscles. *Acta Crystallogr.* D52: 1169–1173.

Yagi, N. 2003. An x-ray diffraction study on early structural changes in skeletal muscle contraction. *Biophys. J.* 84:1093–1102.

Yamada, T., Y. Takezawa, H. Iwamoto, S. Suzuki, and K. Wakabayashi. 2003. Rigor force producing cross-bridges in skeletal muscle fibers activated by a sub-stoichiometric amount of ATP. *Biophys. J.* 85:1741–1753.